Polarized Micro-Raman Spectroscopy of Oriented Microwave $A(B'_{1/3}B''_{2/3})O_3$ Electroceramics

Anderson Dias[a], Roberto L. Moreira[b,*]

[a]*Departamento de Engenharia Metalúrgica e de Materiais, UFMG, Rua Espírito Santo 35, Belo Horizonte-MG, 30160-030, Brazil*

[b]*Departamento de Física, ICEx,UFMG, C.P. 702, Belo Horizonte-MG, 30123-970, Brazil*

Abstract

Complex perovskites of the general formula $A(B'_{1/3}B''_{2/3})O_3$ (A=Ba or Sr, B'=Mg, Mn or Zn and B''=Nb or Ta) belonging to an ordered trigonal structure exhibit remarkable microwave dielectric properties, allowing their use as dielectric resonators. In this spectral region, the dielectric behavior is determined by the phonon characteristics of the materials. In view of these applications and of fundamental studies, ceramic materials are generally obtained and the phonon spectra are then unpolarized, without the benefits of selection rules. In this work we report on our polarized micro-Raman spectroscopy of ordered trigonal $A(B'_{1/3}B''_{2/3})O_3$ ceramics under special experimental conditions. The model system used was $BaMg_{1/3}Nb_{2/3}O_3$ (BMN). The materials were obtained either, by conventional hydrothermal route followed by calcining and sintering or synthesized by microwave-hydrothermal process. The complete assignment of the vibrational modes of BMN ceramics was carried out through the analysis of the dependence of the Raman intensities with light beam polarization beside selection rules predictions. Scanning electron microscopy was employed to show the morphological

characteristics of the hydrothermal powders, as well as to correlate the phonon vibrations with the dielectric properties in the microwave region.

Keywords: A. Powders-chemical preparation; B. Raman spectroscopy; C. Dielectric ceramics; D. Perovskites; E. Microwave resonators

* Corresponding author: Tel.: +55.31.3499.5624; fax: +55.31.3499.5600

E-mail: bmoreira@fisica.ufmg.br

1. Introduction

Some $A(B'_{1/3}B''_{2/3})O_3$ ceramics exhibit suitable microwave and millimeter dielectric responses – such as high values of real dielectric constant, high quality factor and low temperature dependence of the resonant frequency – for use as dielectric resonators in telecommunication devices.[1-4] In these materials, the optical phonons determine the dielectric response, which in turn depends on the morphological structure determined mainly by the experimental preparation conditions.[5] In this respect, the hydrothermal technology appears as the most promising route for environmentally friend and low-cost production of advanced ceramics.[6] A recent innovation in this technology was the introduction of microwaves into the reaction vessels to produce materials with different structural and morphological characteristics from conventional powders.[7,8]

Complex perovskites with general formula $A(B'_{1/3}B''_{2/3})O_3$ can be classified into ordered and disordered types with respect to the degree of long-range order of *B*' (divalent) and *B*" (pentavalent) cations. The disordered materials present a cubic $Pm\bar{3}m$ symmetry. On the other hand, the ordered compounds adopt a trigonal symmetry, owing to a rhombohedral

distortion along a <111> direction of the cubic cell, together with a slight volume increase.[1] The trigonal symmetry is $P\bar{3}$m1, like that of barium strontium tantalate (BST),[1] so that these materials are indexed in terms of hexagonal unit cells. A large number of works have been devoted to BST-type materials because of their high dielectric permittivities and high quality factors in the microwave region.[2-4]

The dielectric response in the millimeter and microwave regions is mainly determined by the characteristics of the optical polar phonons of the material. Thus, the knowledge of the lattice vibrational modes is necessary for describing the dielectric behavior of any material. However, in the case of ceramics, spectroscopic investigations are usually performed with unpolarized light because their intrinsic unoriented nature.[2,3,5,9-14] Then, even in the highly ordered materials were experimental data agree well with group theory predictions, one cannot take benefit of the selection rules, that allow one to distinguish between modes of different symmetries. In the present work, we used samples obtained from different hydrothermal routes, with adequate microstructures, by polarized micro-Raman spectroscopy. Unoriented large and small grained ceramics, as well as oriented and large "needle-like" crystals of barium magnesium niobate were investigated under special experimental conditions and their spectra allowed us to determine the phonon symmetries of the Raman modes. It is straightforward to extend this method to any $A(B'_{1/3}B''_{2/3})O_3$ material.

2. Experiment

Barium magnesium niobates (BMN) were obtained from two different hydrothermal methods. In both cases, the reagents employed were $BaCl_2.2H_2O$, $MgCl_2.6H_2O$ and $NH_4H_2[NbO(C_2O_4)_3].3H_2O$. After the dissolution of each reagent in deionized water, they were mixed (under stirring) and the pH was controlled by adding NaOH to the aqueous

solution until it reached the value 13.5. Conventional hydrothermal powders were produced in an autoclave at 200 °C for 4 hours (20 bar). These powders were calcined at 600 °C and sintered at various temperatures up to 1400 °C. Details about this procedure are given in Ref. 13. Microwave-assisted hydrothermal experiments were performed using a Milestone MLS-1200 MEGA microwave digestion system (2.45 GHz). This system operates at a maximum power of 1000 W, and power can be varied from 0 to 100% controlled by both pressure (autogenous pressure) and temperature. The syntheses occurred in double-walled digestion vessels (100 mL capacity) with an inner line and cover made of Teflon Tetrafluormethaxil (TFM) and an outer high strength vessel shell made of Polyether ether heton (PEEK). The system was programmed to work at 1000 W, for 10 minutes, up to the processing temperature (200 °C) and maintained at 400 W, for 2 hours, for the production of the desired ceramic powders (200±1 °C and 14.7±0.5 bar). After the hydrothermal syntheses, the products were rinsed with deionized water several times and dried at 80 °C.

Chemical analyses were carried out in all produced powders by using atomic absorption spectrometry (Perkin Elmer 5000) and X-ray fluorescence (Philips PW2400 sequential spectrometer, fitted with a Rhodium target end window and Philips Super *Q* analytical software). In order to determine the nature of the crystalline phases, powder X-ray diffraction analyses were performed in a Philips PW1830 diffractometer with Cu$K\alpha$ radiation (40 kV, 30 mA) and graphite monochromator, from 10 to 100°2θ at a speed of 0.02°2θ/s. The morphological properties were determined by using scanning electron microscopy (SEM-JSM6360LV) at 15-25 kV, with energy-dispersive spectrometry (Noran-Voyager 3050 with Norvar detector window and Si-Li X-ray detector crystal).

Polarized micro-Raman scattering spectra were recorded using a *Jobin-Yvon* LABRAM-HR spectrometer equipped with a liquid-N_2-cooled CCD detector and a confocal microscope, with an experimental resolution of 2 cm^{-1}. The measurements were carried out in

back-scattering geometry at room temperature, using the 632.8 nm line of an helium-neon ion laser (power 2 mW) as excitation source. A Notch filter was used to stray light rejection. The sample surfaces of the conventional sintered materials were previously polished to an optical grade in order to improve the ratio of inelastic to elastic scattered light. The normal modes in these perovskites are sensitive to the presence of disordering and local stresses.[5] Therefore, a careful fitting of the Raman peaks was done, leading to an ultimate precision of about 0.2 cm^{-1}. Before fitting, the spectra were divided by the Bose-Einstein thermal factor $[n(\omega) +1]$.[15] The powders synthesized by microwave-hydrothermal process were oriented and carefully examined by polarized micro-Raman spectroscopy.

3. Results and discussions

X-ray diffraction analysis showed the presence of a crystalline and single-phase BMN (indexed by the ICDD card # 17-0173) with no impurities, as verified by X-ray fluorescence and energy-dispersive spectrometry analyses. SEM results showed that the morphology of microwave-hydrothermal powders changed drastically depending upon the reactor used. The powders produced in conventional reactors were formed by nanometer-sized needles (typical length ~20 nm), so that they could be seen only through transmission electron microscopy.[8] After sintering, the materials present a granular structure, as showed in Figure 1a and 1b, for the BMN sintered at 900 °C and 1400 °C, respectively. In these micrographies the magnification was 10,000×. On the other hand, the microwave-hydrothermal powders are formed by large needle-shape materials, with typical length ranging from 10 to 50 μm, as it can be seen in Figure 2 (the magnification here was 1,000×). It is noteworthy to stress the effect of the microwave heating on the morphological properties of BMN ceramics, increasing

the particle size by three orders of magnitude in comparison with particles obtained by conventional heating.[8,13]

The BMN powders obtained from the two methods were analyzed by unpolarized Raman spectroscopy. Figure 3 presents the spectra obtained with a 100× objective, in the spectral region where all characteristic vibrations appear. We note that the spectra look very similar, with the presence of the strong BMN peaks around 100 and 800 cm^{-1} and several other weaker peaks described in Ref. 5. It is worthy to notice that these samples have been produced at 200 °C. Then, despite the enormous difference between their crystal's dimensions, they should both present some disorder of the *B* cations. This could also explain the high peak widths and the relative importance of the peaks around 300 and 580 cm^{-1}, compared to ordered (i.e. sintered) ceramics.[5]

BST-type crystals belong to the trigonal D_{3d}^3 space group ($P\bar{3}m1$), with 15 atoms in the primitive cell.[1] The optical active modes of the ordered ceramics should be those predicted for the single crystal. Their number and symmetries can be determined by group theory tools, as it was done for the isomorphous barium zinc tantalate system by Tamura et al.[2]. In the simplest description, the lattice vibration representation can be obtained by factor-group analysis based on the occupied Wyckoff sites, by using the method of Rousseau et al.[16]. For the ordered BMN material, two Ba ions occupy *2d* sites and one Ba ion sits on a *1b* site, giving $\Gamma_{Ba} = A_{1g} + 2A_{2u} + E_g + 2E_u$; the Mg ion occupies a *1a* site ($\Gamma_{B'} = A_{2u} + E_u$); the two Nb ions are in *2d* sites ($\Gamma_{B''} = A_{1g} + A_{2u} + E_g + E_u$); six O ions are in *6i* sites and three O ions in *3f* sites ($\Gamma_O = 2A_{1g} + 2A_{1u} + A_{2g} + 4A_{2u} + 3E_g + 6E_u$). Three of these modes ($2A_{1u} + A_{2g}$) are silent and after subtracting the acoustic modes ($A_{2u} + E_u$) there remain 9 Raman-active modes ($4A_{1g} + 5E_g$) and 16 Infrared-active ones ($7A_{2u} + 9E_u$). The Raman and IR modes are mutually exclusive, owing to the centro-symmetric nature of the crystal group.

The inelastic scattered light intensities due to the Raman effect are proportional to the square of the elements of the polarizability tensor, a second order tensor. Then, the base functions of the irreducible representations (i.r) that contain the Raman-active modes have a quadratic form, i.e. they transform like the product of the Cartesian coordinates. When dealing with crystals, we take benefit of the crystal symmetry to assign the lattice vibrations to the different i.r..[15,16] However, in the case of ceramics, although the group theory predictions remain valid, the symmetry of modes are generally mixed due to the random orientation of the small crystalline grains. But, what happens when the scattering volume has the same dimensions as the crystalline grains? In this case, for special orientations, the selection rules could be proved.

The confocal microscope with an objective of magnification of 100× allows the selection of an observation region as small as 2 μm on the sample surface or even inside the sample. As it can be seen in Figure 1, the BMN sample sintered at 1400 °C has a grained structure, with crystalline grains slightly larger than 1 μm. Then, this system could be analyzed by polarized Raman spectroscopy. Nevertheless, we do not know anything about the crystallographic axes of these grains, which have also random orientation throughout the sample. In spite of this, we know that all cross-polarized quadratic functions (i.e. xy, xz, yz) are base functions of the E_g i.r. of a group of D_{3d} symmetry (zz relates only to A_{1g}, and xx and yy to both Raman-active i.r.).[15] Then, by measuring the micro-Raman spectra of BMN sample sintered at 1400 °C with cross-polarized light, we displaced the sample under the microscope looking for spectral changes. We observed that for some grains the spectra of parallel and crossed light became different, as exemplified in Figure 4. For different grains, we always observed the relative strengthening of the bands around 175, 265, 298, 387 and 437 cm^{-1} with cross-polarized light, accompanied by the relative weakening of bands at 248, 566, 630, 730, 790 and 833 cm^{-1}. The behavior of the strong band at 105 cm^{-1} is not so simple and will be

analyzed later. We also measured other samples with smaller grains, as exemplified by the BMN sample sintered at 900 °C, in the same figure. In these cases, no difference was depicted between parallel and cross-polarized spectra (except, of course, in the absolute units), which we attribute to the fact that the observation region contains hundreds of small unoriented crystals. Then the effect observed in figure 4 is undoubtedly due to selection rules linked to the orientation of one or few grains inside the observation region.

By observing the variations of the Raman intensities of the mentioned bands at polarized light in different regions of the sample sintered at 1400 °C, we assign them to their respective i.r., as presented in Table 1. We notice that some ambiguities can exist in the case of 105 cm^{-1}, which according to Chia et al.[14] could have mixed A_{1g} and E_g symmetry, and with the bands at 248, 566 and 833 cm^{-1}, which have parallel symmetry but are weaker than the bands assigned as of A_{1g} symmetry (105, 630, 730 and 790 cm^{-1}). Then, we just attribute the existence of these three weaker bands to defects or activation of forbidden modes. Comparing our results of Table 1 with those of Ref. 14, where the authors used unpolarized spectra of mixed $Ba(Mg_{1/3}Ta_{2/3})O_3$ and $Ba(Mg_{1/3}Nb_{2/3})O_3$ ceramics, we have a good agreement in six of the nine Raman modes. Those authors only observe seven bands in BMN. Then, we believe that our direct observation of the mode's symmetry contributes to partially confirm their results, but also extend them by completing the whole spectra.

Since we had success by using polarized light in the ceramic system with micrometer grains, we performed polarized micro-Raman experiments in the hydrothermal microwave assisted BMN micro-needles. We used a small amount of powder, and after scattering the powder over a microscope slide, the needles could be observed individually. Then, we oriented the polarization of the incoming light beam parallel to the needle axis of a chosen micro-crystal. By taking the parallel and crossed lights in this geometry, we did not discern any significant difference in the spectra. By turning the sample under the microscope under

crossed polarization, we could seen the weakening of A_{1g} modes when the sample axis were roughly at 45° of the polarization of the incoming beam, as shown in Figure 5. This result is a clear indication of: i) the spectra are polarized; ii) the needle axis is not the crystallographic z axis of the trigonal structure (because in this case we should have perfect separation of A_{1g} and E_g modes in parallel and crossed polarizations, respectively, when the incoming beam polarization were parallel to the needle axis). Moreover, although it was difficult to obtain the correct angle that shows the maximum polarization of the scattered spectra, we believe that the needle axis could be the [100] direction of the cubic perovskite of the disordered material. Indeed, Ayala et al.[17] have shown that, when measuring a D_{3d} trigonal crystal in its primitive cubic reference axes, after averaging over the four directions of the cubic diagonals, it is possible to observe only the E_g modes, when incoming and outcoming lightbeams (perpendicular each other) are choosen according to the directions of the cubic faces. They also showed that it is not possible to observe the A_{1g} modes alone. From the physical point of view, it is easy to see why the needles could grow in the cubic directions instead to choose the trigonal one. In fact, this sample was produced at a relatively low temperature (200 °C), so the *B*-cation disorder should be very high, which is in agreement with the overall profile of the corresponding Raman spectra.

4. Conclusions

In this work we have shown that under special experimental conditions the group theory predictions for a $A(B'_{1/3}B''_{2/3})O_3$ material (*A*=Ba or Sr, *B*'=Mg, Mn or Zn and *B''*= Ta or Nb) are fully obeyed, even for unoriented ceramic samples. The model system used was hydrothermal-grown BMN samples, an ordered material with trigonal structure. By using observation regions of the same dimensions of the grain size, the polarized Raman spectra

were different for parallel and cross-polarized lights, allowing the assignment of the nine observed Raman bands of BMN into their respective irreducible representations. This result also holds for any compound with BST structure. We also showed that samples obtained by the microwave-assisted method, with dimensions larger than the scattering volumes, present polarized spectra with orientations at 45 degrees of the needle axis. This result allowed us to propose the growth direction (at low temperature) as the [100] direction of the disordered cubic perovskite. This result is particular to this ceramic, but this procedure can be applied to investigate any $A(B'_{1/3}B''_{2/3})O_3$ compound, irrespective of a particular structure.

Acknowledgements The authors acknowledge the financial support from the Brazilian agencies CNPq and MCT (The Millenium Water Institute). They are also pleased to thank Prof. V.S.T. Ciminelli for her hospitality during the Raman experiments.

References

1 Galasso, F. S., *Structure, Properties and Preparation of Perovskite-Type Compounds*. Pergamon Press, Oxford, 1969, pp.13-15, 55.

2 Tamura, H., Sagala, D. A. and Wakino, K., Lattice vibrations of $Ba(Zn_{1/3}Ta_{2/3})O_3$ crystal with ordered perovskite structure. *Jpn. J. Appl. Phys.*, 1986, **25**, 787-791.

3 Sagala, D. A. and Koyasu, S., Infrared reflection of $Ba(Mg_{1/3}Ta_{2/3})O_3$ ceramics. *J. Am. Ceram. Soc.*, 1993, **76**, 2433-2436.

4 Lu, C. H. and Tsai, C. C., Reaction kinetics, sintering characteristics, and ordering behavior of microwave dielectrics: barium magnesium tantalate. *J. Mater. Res.*, 1996, **11**, 1219-1227.

5 Moreira, R. L., Matinaga, F. M. and Dias, A., Raman-spectroscopic evaluation of the long-range order in $Ba(B'_{1/3}B''_{2/3})O_3$. Appl. Phys. Lett., 2001, **78**, 428-430.

[6] Cabanas, A., Darr, J. A., Lester, E. and Poliakoff, M., Continuous hydrothermal synthesis of inorganic materials in a near-critical water flow reactor: the one-step synthesis of nano-particulate $Ce_{1-x}Zr_xO_2$ (x=0-1) solid solutions. *J. Mater. Chem.*, 2001, **11**, 561-568.

[7] Komarneni, S., Roy, R. and Li, Q. H., Microwave-hydrothermal synthesis of ceramic powders. *Mater. Res. Bull.*, 1992, **27**, 1393-1405.

[8] Dias, A. and Ciminelli, V. S. T., Electroceramic materials of tailored phase and morphology by hydrothermal technology. *Chem. Mater.*, 2003, **15**, 1344-1352.

[9] Furuya, M., Microwave dielectric properties and phonon characteristics for $Ba(Mg_{1/3}Ta_{2/3})O_3$-$A(Mg_{1/2}W_{1/2})O_3$ (A=Ba, Sr, and Ca) ceramics. *J. Korean Phys. Soc.*, 1998, **32**, S353-S358.

[10] Youn, H.-J., Hong, K. S. and Kim, H., Far-infrared reflectivity study of $Ba(Mg_{1/3}Ta_{2/3})O_3$-$La(Mg_{2/3}Ta_{1/3})O_3$ complex perovskite ceramics. *J. Korean Phys. Soc.*, 1998, **32**, S524-S526.

[11] Nagai, T., Sugiyama, M., Sando, M. and Niihara, K., Anomaly in the infrared active phonon modes and its relationship to the dielectric constant of $(Ba_{1-x}Sr_x)(Mg_{1/3}Ta_{2/3})O_3$ compound. *Jpn. J. Appl. Phys. (Pt.1)*, 1996, **35**, 5163-5167.

[12] Sagala, D. A. and Nambu, S., Lattice energy calculations for ordered and disordered $Ba(Zn_{1/3}Ta_{2/3})O_3$. *J. Phys. Soc. Jpn.*, 1992, **61**, 1791-1797.

[13] Dias, A., Ciminelli,V. S. T., Matinaga, F. M. and Moreira, R. L., Raman scattering and X-ray diffraction investigations on hydrothermal barium magnesium niobate ceramics. *Journal of the European Ceramic Society*, 2001, **21**, 2739-2744.

[14] Chia, C. T., Chen, Y. C., Cheng, H. F. and Lin, I. N., Correlation of microwave dielectric properties and normal modes of $xBa(Mg_{1/3}Ta_{2/3})O_3$-$(1-x)Ba(Mg_{1/3}Nb_{2/3})O_3$ ceramics: I. Raman spectroscopy. *J. Appl. Phys.*, 2003, **94**, 3360-3364.

[15] Hayes, W. and Loudon, R., *Scattering of Light by Crystals*. Wiley, New York, NY, 1978, pp. 7, 31.

[16] Rousseau, D. L., Bauman, R. P. and Porto, S. P. S. Normal mode determination in crystals. *J. Raman Spectroscopy*, 1981, **10**, 253-290.

[17] Ayala, A. P., Paschoal, C. W. A., Guedes, I., Paraguassu, W., Freire, P. T. C., Mendes Filho, J., Moreira, R. L. and Gesland, J.-Y., "Disorder-induced symmetry lowering in the $CsMgInF_6$ pyrochlore crystal". *Phys. Rev. B*, 2002, **66**, 2141051-2141058.

Table 1. Raman fitting parameters (polarized spectra) and assignments for the BMN sample sintered at 1400 °C (wavenumbers and half widths in cm^{-1}). The intensities are in relative units and were determined independently for parallel (A_{1g}) or cross-polarized (E_g) lights.

Wavenumber	HWHM	Intensities*	Assignment
105	3	64	A_{1g}
175	4	13.5	E_g
265	7	3.3	E_g
298	5	9.0	E_g
387	4	100	E_g
437	6	18	E_g
630	25	6.5	A_{1g}
730	20	8.0	A_{1g}
790	14	100	A_{1g}

* Normalized for the corresponding polarizations.

FIGURES

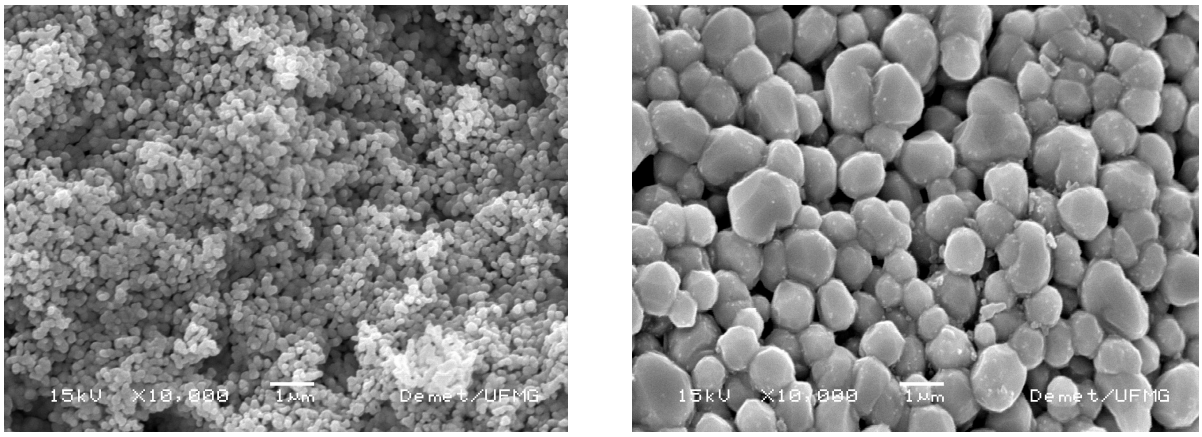

a) b)

FIG. 1. Scanning electron micrographies, under magnifications of 10,000×, of BMN samples obtained by conventional hydrothermal processing at 200 ^{o}C (4 h), calcined at 600 °C and sintered at: a) 900 °C and b) 1400 °C. The scales of the figures are 12.5μm × 9.5μm.

FIG. 2. Scanning electron micrography of a BMN sample (magnification of 1,000×) obtained by microwave-assisted hydrothermal processing at 200 °C for 2 h. The scale of the figure is 125μm × 95μm.

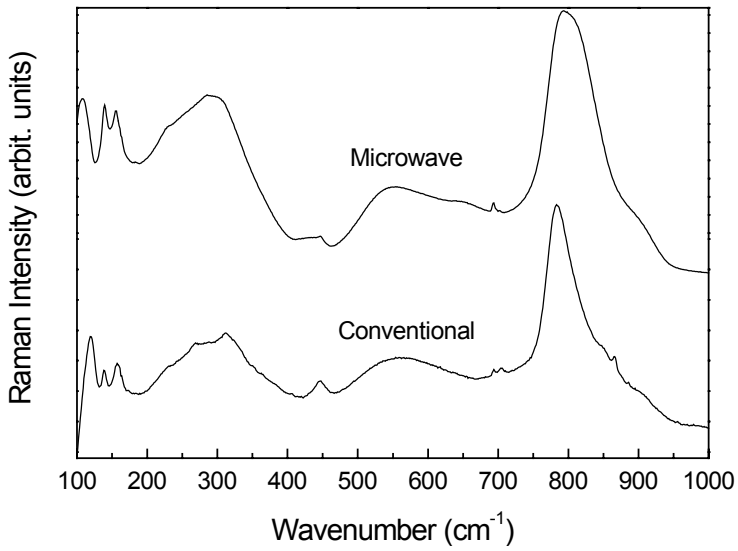

FIG. 3. Unpolarized micro-Raman spectra of microwave-assisted and conventional hydrothermal BMN powders, between 100 and 1000 cm^{-1}.

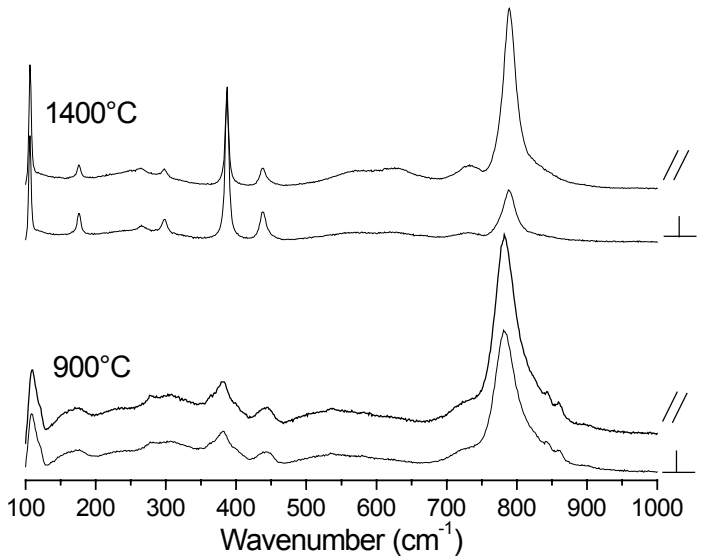

FIG. 4. Parallel and cross-polarized micro-Raman spectra of BMN ceramic samples obtained form the conventional method after sintering at 900 °C (bottom) and 1400 °C (top), obtained with a microscope objective of 100×.

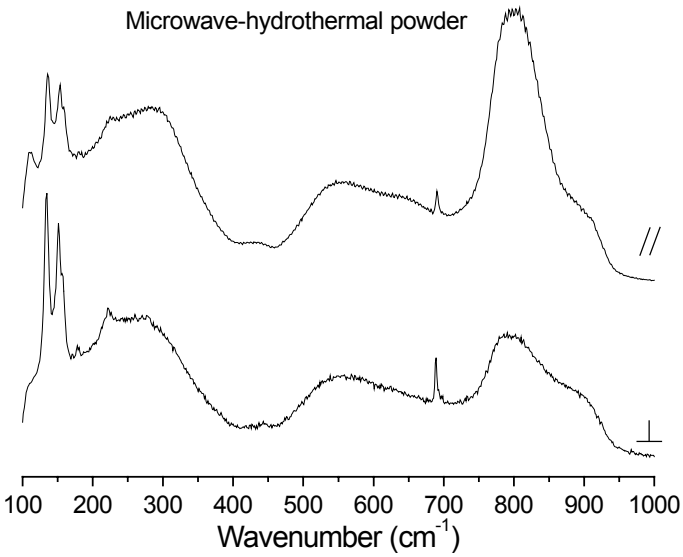

FIG. 5. Parallel and cross-polarized micro-Raman spectra of a BMN sample obtained by microwave-assisted hydrothermal processing, obtained with a 100× objective and with the needle axis at approximately 45 degrees of the incoming-beam polarization.